Fusion Engineering and Design 85 (2010) 1296–1300

Contents lists available at ScienceDirect

Fusion Engineering and Design

journal homepage: www.elsevier.com/locate/fusengdes

Neutronics assessment of the shielding and breeding requirements for FNSF (standard aspect ratio)

Haibo Liu*, Mohamed A. Abdou, Robert J. Reed, Alice Ying, Mahmoud Z. Youssef

Engineering IV 44-139A, Mechanical and Aerospace Engineering Department, University of California, Los Angeles, CA 90095, USA

ARTICLE INFO

Article history:
Available online 11 April 2010

Keywords:
Fusion nuclear science facility
Inboard shielding
Radiation damage
Insulator
Magnet protection

ABSTRACT

This paper presents design and analysis results regarding key aspects of the neutronics for a standard aspect ratio fusion nuclear science facility (FNSF). Optimization of the inboard design is based on maximizing tritium production and minimizing radiation damage to the ohmic heating coil (OHC). The calculations show that the outboard tritium breeding blanket alone is not enough for achieving tritium self-sufficiency in the FNSF. Options to enhance tritium production in FNSF include the use of either a thin, specifically designed tritium breeding blanket or the use of only a multiplier in the highly space-constrained inboard region. Trade-offs between breeding, shielding to protect the magnets, and materials for the inboard region shows that an inboard thickness of 50 cm is enough if a ceramic insulator is used. If an organic insulator is preferred, the inboard thickness has to be increased. Radiation-induced increase in the electrical resistivity of the copper has also been studied and its impact on the aforementioned optimization process for the blanket/shield thickness/material choice has been accounted for.

Published by Elsevier B.V.

1. Introduction

A fusion nuclear science facility (FNSF) is being evaluated for resolving key issues of fusion nuclear science and technology (FNST) that can not be fully addressed by ITER, such as tritium self-sufficiency and engineering feasibility and reliability of the FW/Blanket components. Because of the tritium supply issue, this facility has to be small size, low Q, low power, and use of normal magnets [1–3]. Reducing the IB thickness makes it possible to reduce the size of the reactor for the same reactor power [4]. In this paper, we explore a FNSF based on General Atomics' preliminary fusion development facility (FDF) design [5]. The tritium breeding ratio (TBR) is maximized for this machine with a fixed IB shielding thickness of 50 cm. This machine has a standard aspect ratio of 3.5 and a normal copper magnet system. The major radius is 2.5 m and the plasma elongation is 2. The OHC is located inside the inner toroidal field coil (TFC), as shown in Fig. 1. This is a 20 degree model with reflective boundary conditions in the toroidal direction. The assumed peak inboard (IB) neutron wall load is 2 MW/m^2 and the peak IB neutron fluence is assumed to be 6 MWa/m^2. MCNP and the FENDL/MC-2.1 cross section library are used for this work [7,8].

The midplane radial dimensions from outer-torus to in-torus are as follows, 83.4 cm outboard (OB), 132 cm plasma chamber, 50 cm IB, 2 cm VV, 0.2 cm insulator and 7.8 cm OHC. The OB blanket assumes DCLL breeding modules [9]. Three PbLi breeder channels are used with radial dimensions of 21.1 cm, 19.6 cm, and 19.6 cm, respectively. The OHC is comprised of 60% copper, 25% water and 15% insulator. Both organic epoxy and ceramic spinel ($MgAl_2O_4$) insulators are evaluated. To investigate the worst case, the vacuum vessel (VV) is voided in order to explore more conservative OHC damage rates.

2. Shielding effectiveness

Table 1 summarizes the IB configurations for the five cases analyzed in the present study. Both the tritium breeding and shielding effectiveness are important to the IB design. PbLi is used in the IB and OB as the tritium breeder. The lithium in PbLi is 90% enriched with ^{6}Li. For the shielding material, the composition of the homogenized mixture is as follows: 5% H_2O, 5% stainless steel (SS), 25% B_4C and 65% W. Here tungsten and iron are good attenuators for high energy neutrons and gamma rays; the carbon and water are used for moderating the neutrons below the inelastic scattering threshold of tungsten and iron; boron is a strong neutron absorber and leads to reduction of the radiative capture reactions [4]. The first wall (FW) consists of 40% ferritic steel (FS) and 60% helium. The reflector is made of 100% FS.

The dimensions of the breeder and multiplier are based mainly on the mean free path of neutrons in the materials, as shown in Table 1. Case 1 has 7 cm of PbLi to evaluate the tritium breeding capability without a beryllium multiplier. Case 2 only has 5 cm of beryllium in order to evaluate if the IB is capable of just multiply-

* Corresponding author. Tel.: +1 310 794 7323; fax: +1 310 825 2599.
E-mail address: haibo@fusion.ucla.edu (H. Liu).

0920-3796/$ – see front matter. Published by Elsevier B.V.
doi:10.1016/j.fusengdes.2010.03.023

Table 1
Inboard blanket/shield configuration.

Case	FW (cm)	Breeder/Multiplier (cm)	Reflector (cm)	Shield (cm)
1	2	PbLi (7)	FS (5)	36
2	2	Be (5)	FS (5)	38
3/5	2	PbLi (2) + Structure (0.5) + Be (5) + Structure (0.5) + PbLi (5)	FS (5)	30
4	2	PbLi (2) + Structure (0.5) + Be (3) + Structure (0.5) + PbLi (5)	FS (5)	32

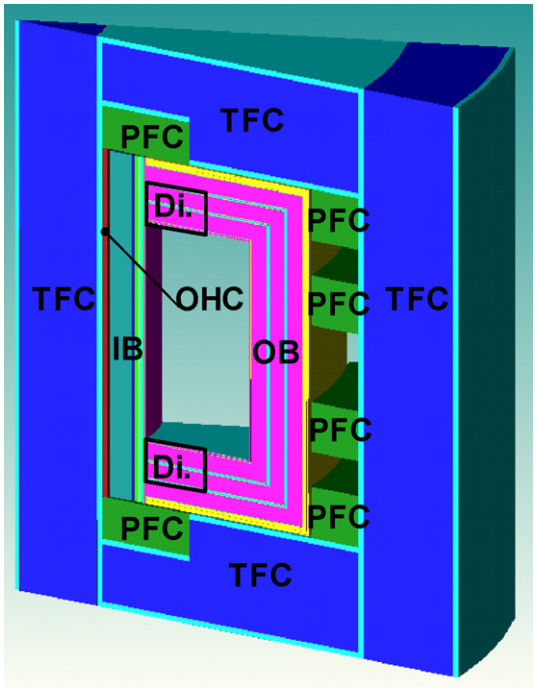

Fig. 1. FNSF CAD model from MCAM [6].

ing and reflecting more neutrons to the OB for tritium breeding. Case 3 has a "sandwiched" configuration for the Be multiplier, i.e. of PbLi + Be + PbLi, which is an optimization of tritium breeding, neutron multiplying, and shielding [10,11]. In the "sandwiched" configuration, the first 2 cm of PbLi reacts with reflected neutrons from the beryllium for enhanced tritium breeding. Case 4 is used to check the effectiveness of a beryllium multiplier. Case 5 has the same inboard configuration as the third case, but Case 5 has a full coverage OB, meaning the OB extends into the divertor region, as shown in Fig. 1. In this case, the tokamak height has to be increased to account for the divertor region.

All of the cases have 5 cm of FS as a reflector. The remainder of the space is filled with shielding with the material composition mentioned above.

3. Tritium breeding analysis

The TBR results are given in Table 2. The first case has a total TBR of 0.901 with an IB TBR fraction of 10% (0.091). The second case, with a pure multiplier in the IB, increases the OB TBR by 6% (compared to Case 1) because of the reflected neutrons from the IB. However, it only amounts to a total TBR of 0.86. Case 2 proves that relying

Table 2
Tritium breeding ratio.

	Case 1	Case 2	Case 3	Case 4	Case 5
IB TBR	0.091	0	0.21	0.16	0.21
OB TBR	0.81	0.86	0.83	0.83	1.03
Total TBR	0.901	0.86	1.04	0.99	1.24

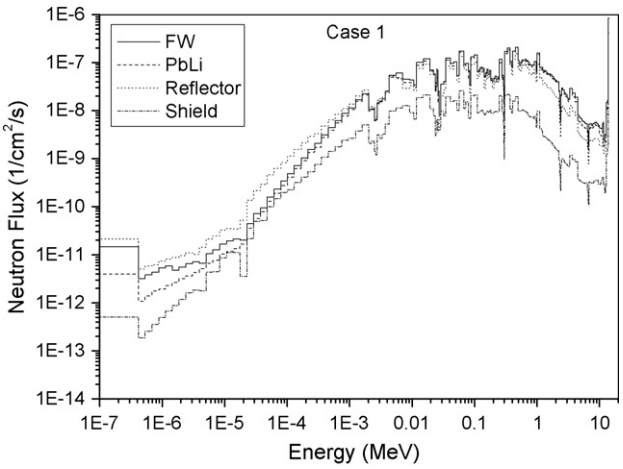

Fig. 2. Region averaged neutron flux for Case 1.

only on OB tritium breeding is not enough, even with a multiplier in the inboard. Both cases also show that both IB and OB breeding and neutron multiplication have to be utilized simultaneously. The third case, using the "sandwiched" configuration, has a total TBR of 1.04. The IB contribution to the total TBR is ~ two times higher than the corresponding contribution in case 1, with a value of 0.21. This is because of the dramatically increased neutron flux and the large ^{6}Li (n, t) cross section in low and intermediate energy range with the IB "sandwiched" configuration, as flux spectra shown in Figs. 2 and 3. The total TBR can be further increased to 1.24 by extending the OB tritium breeding blanket into the divertor region, as shown in Case 5. Case 4 has a smaller IB TBR compared to Case 3 because of the 2 cm decrease of the IB multiplier. So 2 cm beryllium may distinctly affect the IB TBR. In this calculation, full coverage of FW is assumed, without consideration of penetration from like heating and current drive (H&CD) system. So the real TBR may be lower than calculated, but the following calculation shows that the

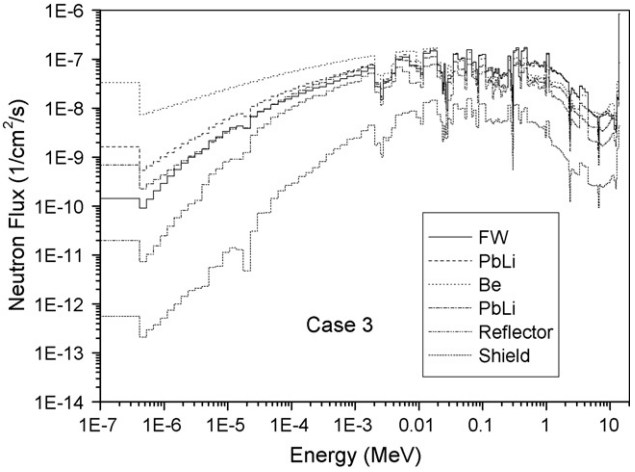

Fig. 3. Region averaged neutron flux for Case 3.

appropriate magnet insulator choice can give much more spaces for optimization of TBR and hence compensate the effect from H&CD system.

4. Damage rates

The end-of-life helium production in the VV structure should be limited to 1 appm to allow for rewelding [12]. The helium production rates in all five cases are below 1 appm when reaching a neutron fluence of 6 MWa/m^2. The maximum value is found in Case 5 with a 0.33 He appm, which means that there is no problem of reweldability of the VV during the lifetime of the FNSF.

The present analysis reveals that the DPA in the copper of the OHC is not sensitive to the insulator choices. The largest one is from Case 5 with a value of 0.05 DPA at the neutron fluence of 6 MWa/m^2. The copper, or copper alloys, will suffer from severe radiation embrittlement when irradiated at temperatures less than 100 °C for doses above 0.01–0.1 DPA. However irradiation at temperatures above 150 °C causes only moderate embrittlement for doses up to approximately 5 DPA [13–17]. If the FNSF copper magnet can be operated around 150 °C, the embrittlement from a dose of 0.05 DPA would not be a concern during its lifetime. Also, the OHC can be designed to handle extra stress in order to avoid coil failure from copper embrittlement.

There are two contributions to the copper magnet electrical resistivity change: radiation defects and transmutation [18–20]. For radiation defect-induced electrical resistivity change, $\Delta\rho_{\mathrm{rad,def}} \approx A \times (1 - \mathrm{Exp}[-B \times \mathrm{DPA}])$ is used, where A is the saturation electrical resistivity change. $A = 1.2$ nΩm for pure copper at 100 °C, and $B = 100$ [21,22]. For the transmutation component, which is proportional to neutron fluence, $\Delta\rho_{\mathrm{tr}} \approx K_{\mathrm{Ni}}C_{\mathrm{Ni}} + K_{\mathrm{Zn}}C_{\mathrm{Zn}}$, where $K_{\mathrm{Ni}} = 11.2$ nΩm, $K_{\mathrm{Zn}} = 3.0$ nΩm, and C_{Ni} and C_{Zn} are atomic percentages [18,19]. The electrical resistivity of pure copper is 17.1 nΩm at 20 °C.

In this calculation, the electrical resistivity change is not sensitive to either the insulator choice or the different cases under consideration. The main contribution is from DPA-induced electrical resistivity change and it pushes the value close to the saturation value of 1.2 nΩm. The transmutation-induced resistivity change is small because of the low neutron fluence. The total electrical resistivity change is about 1.2 nΩm, a 7% increase to the total copper electrical resistivity. The resistivity increase will induce Joule loss and also redistribute the OHC current density [15,17,22,23]. Since much of the DPA-induced electrical resistivity increase could be annealed at the copper operating temperature, the real resistivity change for FNSF operation should be smaller.

The dose rates were calculated for the two types of insulators. In FNSF, the dose rate for the epoxy insulator is much higher than the limit of 10^7 Gy [24]. The minimum is found in Case 2 because of the larger shielding thickness, with a dose rate of 3.6×10^8 Gy. Therefore, the ceramic insulator is suggested for the FNSF OHC, which has dose limit 2–3 orders of magnitude higher than the organic insulators. The magnesium aluminate spinel ($MgAl_2O_4$) is one of the most radiation-resistant ceramic insulators known and has been used for American MARS and TITAN tokamak magnet designs [25–29].

The fluence limit for cubic spinel is determined by the maximum swelling limit that the magnet design can tolerate [30]. A maximum swelling of 3% is used for this calculation [23,31]. The reported irradiation swelling data for $MgAl_2O_4$ indicates a swelling of approximately 0.8 vol% for a fast fission irradiation of 2.1×10^{26} n/m^2 at 430 K [27,32]. Therefore, with the conservative assumption that the fusion neutron spectrum will enhance the swelling rate by a factor of two, the maximum tolerable fast neutron fluence is 3.9×10^{26} n/m^2 [23,30,33]. Fig. 4 shows the dose rates of the ceramic insulator for the five studied cases. For an IB

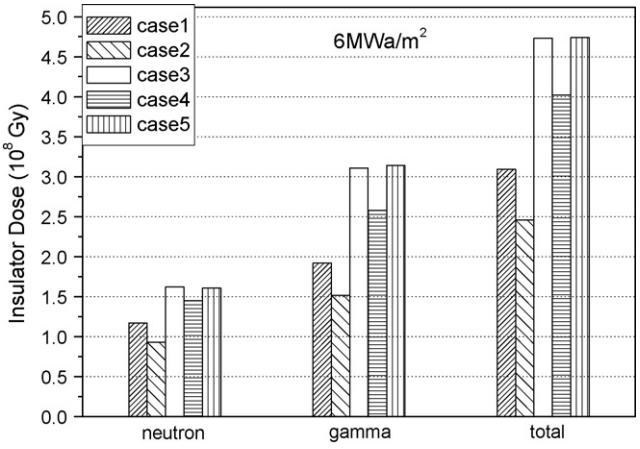

Fig. 4. Peak dose with spinel insulator.

fluence of 6 MWa/m^2, the maximum dose rate to the spinel insulation is 4.7×10^8 Gy in Case 5, corresponding to a 4.7×10^{23} n/m^2 fast neutron fluence (1×10^{15} n/m^2 results in approximately 1 Gy for energies greater than 0.1 MeV) [24]. This is three orders of magnitude lower than the tolerable fast neutron fluence. It follows that if a ceramic insulator is used, the IB blanket could be further optimized to achieve a higher TBR by increasing the PbLi layer thickness and decreasing the shielding layer thickness. The Case 3 has almost the same damage rates with Case 5 because of the same IB configuration.

5. Nuclear heating rate

Figs. 5 and 6 show the nuclear heating rate along the midplane of the IB for Case 1 and Case 5, respectively. In Case 1, the FW peak heating rate is about 15 W/cm^3. For the PbLi layer, the heating rate decreases in the first 5 cm and then increases for the next 2 cm because of the reflected neutrons from the FS. The lead helps to multiply the neutrons through the Pb (n, $2n$) reaction. The peak heating for the PbLi layer is about 17 W/cm^3, 75% of which comes from gamma energy. After the total IB thickness (50 cm) the nuclear heat drops below a value of 0.04 W/cm^3 in Case 1, and the main contribution comes from gamma energy deposition. The peak nuclear heating rate in Case 5 is about 16 W/cm^3 in the FW-FS. There is obvious neutron multiplication and reflection from the beryllium multiplier in the first PbLi layer of Case 5, which makes the peak

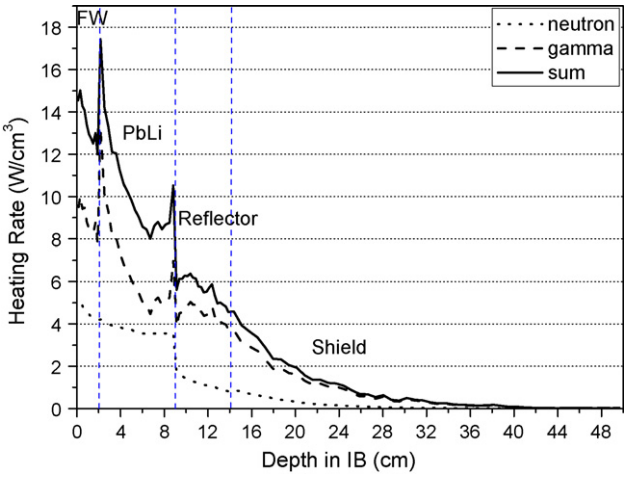

Fig. 5. Nuclear heating for Case 1.

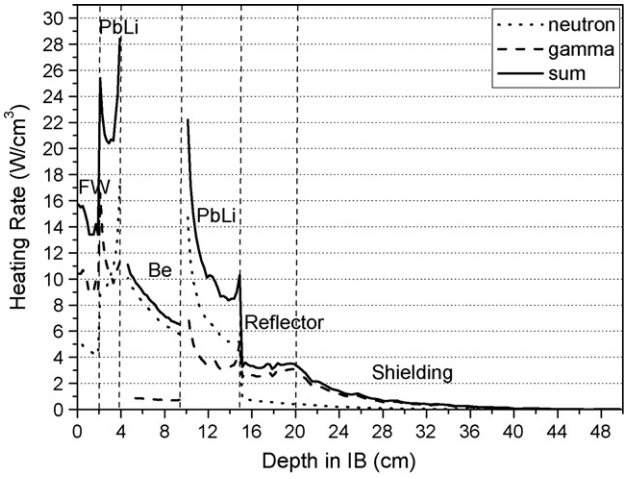

Fig. 6. Nuclear heating for Case 5.

nuclear heating about 28 W/cm^3 in this layer. The neutron energy deposition becomes dominant along the first PbLi layer radial depth because of the multiplication of neutrons from beryllium. In the beryllium layer, the nuclear heating comes mainly from the neutrons because of the small Be (n, γ) cross section at intermediate and high energies. In the second PbLi layer, the neutron energy deposition counts for two-thirds of the contribution to the total heat due to the effect from the multiplier. After the total IB thickness (50 cm) the nuclear heat drops below a value of 0.032 W/cm^3 in Case 5. The third case should have almost the same nuclear heat distribution as Case 5, since they have the same IB configurations at the midplane.

6. Summary

Five FNSF IB designs, each with a total IB thickness of 50 cm, have been modeled. In order to achieve tritium self-sufficiency, the PbLi + Be + PbLi "sandwiched" IB design with full OB coverage (Case 5), is the best choice. The TBR from the fifth case is 1.24, which is larger than the other cases. The DPA-induced increase in magnet electrical resistivity is the dominant part of the total increased resistivity under the low neutron fluence. The analysis reveals that the DPA in the copper magnet and helium production rate in the VV are not the life-limiting radiation damage effects for standard aspect ratio FNSF. For Case 5 (and Case 3), the peak nuclear heating rate is found in the first PbLi layer, with a peak value of 28 W/cm^3.

Our study shows that the use of an organic insulator necessitates the inboard shielding thickness to be increased in order to reach allowable dose rates. This is not the case for the ceramic insulators since higher dose rates can be tolerated without degradation in its properties. The $MgAl_2O_4$ would be a good insulator choice for FNSF based upon its good mechanical and electrical properties. It could allow for the inboard design to be further optimized to increase the IB TBR, which may compensate for TBR decreasing effects from the tokamak H&CD system.

Acknowledgement

Work supported by the US Department of Energy.

References

[1] Mohamed A. Abdou, Sam E. Berk, Alice Ying, Y.K. Martin Peng, Shahram Sharafat, John D. Galambos, Glenn W. Hollenberg, Siegfried Malang, Eric Proust, Steven J. Booth, Luciano Giancarli, Patrick Lorenzetto, Yasushi Seki, V.V. Filatov, Guelli Shatolov, Alexander Sidorenkov, Results of an international study on a high-volume plasma-based neutron source for fusion blanket development, Fusion Technology, vol. 29, Jan 1996.

[2] E.T. Cheng, Y.K. Martin Peng, Ralph Cerbone, Paul Fogarty, John D. Galambos, E.A. Mogahed, Brad Nelson, Massoud Simnad, Igor Sviatoslavsky, Mark Tillack, Study of a spherical tokamak based volumetric neutron source, Fusion Engineering and Design 38 (1998) 219–255.

[3] S.K. Ho, M.A. Abdou, Exploration and assessment of design windows for a Tokamak-based volumetric neutron source, Fusion Engineering and Design 31 (1996) 323–332.

[4] Mohamed A. Abdou, Nuclear design of the blanket/shield system for a tokamak experimental power reactor, Nuclear Technology, vol. 29, April 1976.

[5] R.D. Stambaugh, Normal aspect ratio features, readiness, and issues of FNSF. American National FNST Meeting, UCLA 18–20 August 2009.

[6] Y. Wu, FDS Team, CAD-based interface programs for fusion neutron transport simulation, Fusion Engineering and Design 84 (2009) 1987–1992.

[7] X-5 Monte Carlo Team, MCNP-A general Monte Carlo N-Particle Transport Code, Version 5, vol. II: Users Guide, LA-CP-03-0245, Los Alamos National Laboratory, April 2003.

[8] D.L. Aldama, A. Trkov, FENDL-2.1, Update of an evaluated nuclear data library for fusion applications, Report INDC(NDS)-467, International Atomic Energy Agency (2004).

[9] M.Z. Youssef, N.B. Morley, M. Dagher, Impact of The SiC FCI In The DCLL Blanket Module on The Nuclear Environment Inside a Demo Reactor Configuration, presented at the 23rd Symposium on Fusion Engineering, SOFE-09, May 31–June 5, 2009, San Diego, CA, USA, 2009.

[10] M.A. Abdou, H. Maekawa, Y. Oyama, M. Youssef, Y. Ikeda, A. Kumar, C. Konno, F. Maekawa, K. Kosako, T. Nakamura, E. Bennett, Japan Atomic Energy Research Institute/United States Integral Neutronics Experiments and Analyses for Tritium Breeding, Nuclear Heating, and Induced Radioactivity, Fusion Technology, vol. 28, Aug. 1995.

[11] M.Z. Youssef, A. Kumar, M.A. Abdou, Y. Oyama, C. Konno, F. Maekawa, Y. Ikeda, K. Kosako, M. Nakagawa, T. Mori, H. Maekawa, Fusion Integral Experiments and Analysis and the Determination of Design Safety Factors-II: Application to the Prediction Uncertainty of Tritium Production Rate From the U.S. DOE/JAERI Collaborative Program on Fusion Blanket Neutronics, Fusion Technology, vol. 28, Sep. 1995.

[12] ITER Nuclear Analysis Report (NAR), G 73 DDD 2 W 0.2 July, 2004.

[13] S.A. Fabritsiev, A.S. Pokrovsky, S.J. Zinkle, D.J. Edwards, Low-temperatue radiation embrittlement of copper alloys, Journal of Nuclear Materials 233–237 (1996) 513–518.

[14] S.A. Fabritsiev, S.J. Zinkle, B.N. Singh, Evaluation of copper alloys for fusion reactor divertor and first wall components, Journal of Nuclear Materials 233–237 (1996) 127–137.

[15] Laila A. El-Guebaly, The ARIES Team, ARIES-ST nuclear analysis and shield design, Fusion Engineering and Design 65 (2003) 263–284.

[16] S. Sharafat, M. Abdou, M. Youssef, Assessment of advanced copper alloys for normal conducting coils, ICFRM 9 Colorado Springs, 1999.

[17] W. Reiersen, F. Dahlgren, H.-M. Fan, C. Neumeyer, I. Zatz, The ARIES Team, The toroidal field coil design for ARIES-ST, Fusion Engineering and Design 65 (2003) 303–322.

[18] S.A. Fabritsiev, A.S. Pokrovsky, The effect of neutron irradiation on the electrical resistivity of high-strength copper alloys, Journal of Nuclear Materials 249 (1997) 239–249.

[19] S.A. Fabritsiev, A.S. Pokrovsky, S.J. Zinkle, A.F. Rowcliffe, D.J. Edwards, F.A. Garner, V.A. Sandakov, B.N. Singh, V.R. Barabash, The effect of neutron spectrum on the mechanical and physical properties of pure copper and copper alloys, Journal of Nuclear Materials 233–237 (1996) 526–533.

[20] S.J. Zinkle, S.A. Fabritsiev, Copper alloys for high heat flux structure applications, Atomic and plasma-material interaction data for fusion (supplement to the journal Nuclear Fusion) Volume 5, IAEA, Vienna, 1994.

[21] M.A. Abdou, Radiation considerations for superconducting fusion magnets, Journal of Nuclear Materials 72 (1 and 2) (March 1978).

[22] Mohamed E. Sawan, H.Y. Khater, S.J. Zinkle, Nuclear features of the fusion ignition research experiment (FIRE), Fusion Engineering and Design 63–64 (2002) 547–557.

[23] L. John Perkins, Materials considerations for highly irradiated normal-conducting magnets in fusion reactor applications, Journal of Nuclear Materials 122 and 123 (1984) 1371–1375.

[24] Annex to Design Requirements and Guidelines Level 1 (DRG1), Structural Material Database, Article 5. Radiation Limits on Magnets, n 11 FDR 51 01-07-12 R 0.1.

[25] S. Sharafat, N.M. Ghoniem, E. Cheng, P.I.H. Cooke, S. Grotz, R. Martin, F. Najmabadi, C.P. Wong for the TITAN Research Group, Structure and insulator material choices for the titan reversed-field-pinch reactor study, Proc. 12th IEEE Symposium on Fusion Engineering (Monterey, CA, October 1987), IEEE No. 87CH2507-2 IEEE, Piscataway, NJ 1046-1049, 1987.

[26] F.W. Clinard JR., G.F. Hurley, L.W. Hobbs, D.L. Rohr, R.A. Youngman, Structural performance of ceramics in a high-fluence fusion environment, Journal of Nuclear Materials 122 and 123 (1984) 1386–1392.

[27] Linn W. Hobbs, Frank W. Clinard Jr., Steven J. Zinkle, Rodney C. Ewing, Radiation effects in ceramics, Journal of Nuclear Materials 216 (1994) 291–321.

[28] Shahram Sharafat, Nasr M. Ghoniem, Patrick I.H. Cooke, Rodger C. Martin, Farrokh Najmabadi, Kenneth R. Schultz, Clement P.C. Wong, the TITAN Team,

Materials analysis of the TITAN-I reversed-filed-pinch fusion power core, Fusion Engineering and Design 23 (1993) 99–113.
[29] D.S. Tucker, T. Zocco, C.D. Kise, J.C. Kennedy, Effects of neutron-irradiation on $MgAl_2O_4$ and Al_2O_3, Journal of Nuclear Materials 141–143 (1986) 401–404.
[30] L. El-Guebaly, L.J. Perkins, C.W. Maynard, MARS axicell radiation damage and shielding analysis, Nuclear Technology/Fusion 4 (1983) 1171, UWFDM-506.
[31] M.E. Sawan, R.R. Peterson, S. Yu, Shielding analysis for a heavy ion beam chamber with plasma channels for ion transport, Fusion Engineering and Design 51–52 (2000) 1137–1142.
[32] J.L. Scott, F.W. Clinard Jr., F.W. Wiffen, Special purpose materials for fusion application, Journal of Nuclear Materials 133 and 134 (1985) 156–163.
[33] F.W. Clinard Jr., Ceramics for applications in fusion systems, Journal of Nuclear Materials 85 and 86 (1979) 393–404.